Evaluation of a water network's energy potential in dynamic operation

Gautier Hypolite, Olivier Boutin, Sandrine Del Sole, Jean-François Cloarec, Jean-Henry Ferrasse

Evaluation of a water network's energy potential in dynamic operation

Gautier Hypolite[a,b], Olivier Boutin[a], Sandrine Delsole[b], Jean-François Cloarec[b], Jean-Henry Ferrasse[a,*]

[a]*Aix Marseille Univ, CNRS, Centrale Marseille, M2P2, Marseille, France*
[b]*Société du Canal de Provence, Le Tholonet - CS70064, 13182 Aix-en-Provence Cedex 5, France*

Abstract

To address the challenges of the energy transition, reducing consumption and optimizing energy production is crucial for all industrial sectors. In the future, water issues will be as important as energy issues, making the optimization of water supply systems critical. The water sector represents large energy consumption for pumping and heating. In regards to this consumption, water systems have a great potential for energy recovery through hydroelectric production or thermal energy recovery. This article aims to quantify the energy potential of water supply systems, which has not been well understood until now. The energy potential of these systems encompasses hydropower recovery and thermal potential, including heat recovery and cold recovery. For that, a method is developed to estimate this potential, including the recoverable power, its location, and its temporal variation. The method can be used for hydroelectricity production, as well as for heat and cold recovery. The results indicate a hydraulic potential of 15 $MWh.km^{-1}.year^{-1}$, and respectively 1650 $MWh.km^{-1}.year^{-1}$ for heat recovery and 766 $MWh.km^{-1}.year^{-1}$ for cold recovery.

Keywords: Water system energy recovery, Energy efficiency, Water system analysis, Thermal energy, Dynamic modeling

1. Introduction

The abundant use of fossil fuels, initiated by coal mining and then by oil and gas exploitation, is no longer sustainable because of the significant greenhouse gas emissions and the limited availability of resources. In addition to a significant reduction in energy consumption, it is necessary to transition towards low-carbon and highly efficient energy systems. Among energy uses, thermal uses account for a significant share of primary energy consumption (45% for France [1]). Therefore, these uses play an important role in the energy transition. Improving the performance of heat

*Corresponding author
Email address: jean-henry.ferrasse@univ-amu.fr (Jean-Henry Ferrasse)

pumps (HP) is a solution for reducing primary energy consumption in heat production. Currently, air/air heat pumps represent more than 75% of the installed equipment, but these systems have significantly lower efficiency than air/water systems [2]. The same applies for cooling applications, and therefore, the use of water as a hot reservoir improves the systems' efficiency. Identifying low-temperature heat sources (or sinks) for air/water heat pump operation is therefore an important issue. Potential heat sources include sewage systems, seawater, groundwater, drinking water, or air [3].

In this study, the focus is on the potential of pressured water network (drinking water or raw water network) for energy production. In addition to being utilized as heat source, energy can also be recovered from pressurized water system in the form of hydropower.

Indeed, water supply systems, which have been underutilized, have the potential to generate significant energy from the large volumes of water they transport. This article presents a new method for evaluating the available energy, both thermal and hydropower, in a water system, which remains unknown. The method introduces several novelties, including the ability to (i) evaluate the energy potential of an entire network, (ii) consider temporal and spatial variations of the potential, and (iii) account for constraints on water pressure and temperature, as well as the dynamic operation of the network. To overcome these challenges, the method is based on a recursive algorithm that has been developed to compute the available energy. The water supply systems potentials are hydropower recovery (1.1) and thermal potential, which consist of heat recovery (1.2) and cold recovery (1.3).

1.1. Hydropower recovery

Energy uses for water systems operation represent a significant part of global energy usage, accounting for approximately 6 % of global energy uses [4, 5]. Thus, water systems have a significant role in climate change mitigation. The water systems' energy efficiency can be increased by optimizing the sizing and control of networks and pumping stations and by reducing leaks [4].

The average energy intensity of water systems has been used as a metric to evaluate improvements in energy efficiency [6]. However, this method does not consider the temporal and spatial variability of water flow and pressure. Liu and Mauter [7] propose using a new metric, called the "marginal energy intensity" (MEI),which they defined as "the energy intensity of the next unit of water consumed at a specific location and time." They compute the MEI values over a network using a flow backtracking algorithm.

Hydroelectric power generation on the networks can also be considered to improve water system efficiency. To this day, in most networks, pressure reduction is obtained using pressure breaking valves [8]. However, hydro-energy recovery from water systems shows a high potential [9, 10, 11, 12, 13].

Although small hydro-power plant have been considered [10], the use of Pumps As Turbines (PAT) has been studied recently by numerous authors [14, 15, 16, 12] to mitigate the expensive cost of a hydropower plant. The use of pumps as turbines allows recovering energy by replacing pressure-reducing valves with a lower cost than turbines [8]. Tricarico et al. [17] propose to minimize the surplus pressure at the network node to optimize the water system operation. The optimal operation is obtained by reducing pumping cost and maximizing energy recovery. The optimization is performed using an evolutionary algorithm. The integration of PAT in a dynamic

model has been studied by De Marchis et Freni [18, 19] to represent the water supply system modifications.

The plant location is a key parameter in the plant efficiency, Mohammadi et al. [20] give a method based on cost, maintenance, and hydraulic attributes to select the optimal plant location. The evaluation of water flow and pressure according to time is another issue that has been raised [14]. For this purpose, dynamic modelization of water system can be performed to determine flow and pressure [10, 17, 12].

While many studies have looked at energy recovery, the full system potential has not been fully studied. In this paper, a new method to evaluate the available energy of a water system is presented. The novelty of the method, is to evaluate the energy potential according to time and location using a recursive algorithm. The method uses value of flow rate and pressure as input, both are already computed thanks to available software such as Epanet. The consideration of the time and location-based variability of the system energy intensity is a major improvement proposed by our method. Indeed, as it was highlighted by Liu and Mauter [7], the spatial and temporal variability of water system energy intensity is a limitation to energy efficiency improvement.

1.2. Heat recovery for heating

In addition to power recovery, thermal energy can be recovered from water supply systems. The recovery of thermal energy from raw water has been identified and tested in South Korea [21].

Cho and Yun [21] describe the installation of heat pumps for heating and cooling in the city of Cheongju. They suggest using raw water as a source instead of outdoor air because water is warmer than air in winter and colder in summer. The COP obtained is 3.3 for the heating season and 7.2 for the air conditioning season. Oh et al. [22] suggest integrating a heat pump, whose heat source is raw water system, for heating and cooling a water treatment plant. The aim was to study the system's operation, they obtain a COP of 4.2 for the annual operation, showing that, the use of raw water as a heat source provides a significant improvement compared to an air source heat pump with a typical COP value below 3 [2].

The other thermal use of pressurized water networks concerns drinking water systems. Kılkıs [23] suggests a method to improve urban system performance including heat recovery from drinking water system. The energy recovered using a heat pump can then be distributed through an urban heating network [24]. The use of a heat pump using drinking water as a heat source has been investigated in the Netherlands by Blokker et al. [25], in Italy by De Pasquale et al. [26], in Denmark by Hubeck-Graudal et al. [27], and in Poland by Piotr and Elżbieta [28]. The challenge in these studies is to assess the benefits of heat production with a heat pump, using a drinking water network as a heat source. For the studies concerning Netherland, Italy, and Denmark, the water supply systems are modeled with the software Epanet [29] to evaluate water flow, and with Epanet MSX [30] to assess water temperature evolution in the network.

Blokker et al. [25] propose to heat 900 houses in the city of Almere in the Netherlands with a drinking water heat pump system, which would result in an annual production of 11.5 $GWh.year^{-1}$. The quantity of water flowing in the system is not desrcibed. The drinking water temperature decreases by 1.16°C in the heat pump. The water temperature evolution in the network after the exchange is calculated assuming that the presence of pipes does not affect the ground temperature. The use of the heat pumps results in an average decrease of 0.125°C at the consumers' taps. As

part of the water is heated before use, reducing the temperature at the tap leads to an increase in consumers' energy consumption. Blokker et al. [25] estimate that the additional energy needed to heat the water is 851 $MWh.year^{-1}$, which represents 7% of the energy produced by the heat pump. They evaluate that the CO_2 emissions reductions obtained with the system are 30 % compared to the reference scenario (heating with a gas boiler).

For the city of Milan in Italy, De Pasquale et al. [26] are studying a 4.9 MW heat pump installation on the drinking water network, in which a mean flow of 314 $L.s^{-1}$ circulates. The exchange led to a temperature reduction of 3°C for the water entering the network. In this case, the reduction in temperature at consumers' tap leads to an increase in energy consumption for water heating of 3.6 $GWh.year^{-1}$, which corresponds to 30 % of the energy produced by the heat pump.

Hubeck-Graudal et al. [27] are studying a similar system for the city of Copenhagen in Denmark to produce 35.9 MW of heat with a network carrying a mean flow of 1366 $L.s^{-1}$. Here, the energy required for water heating corresponds to 29 % of the energy extracted by the heat pump. Considering this additional energy requirement, the equivalent COP of the entire system is 1.7. Hubeck-Graudal et al. [27] conclude that the system should only be considered when there are no other heat sources available.

Piotr and Elżbieta [28] suggest recovering up to 3.9 $GWh.year^{-1}$ in the water system of the city of Głogow in Poland; the flow in the system varies between 55 $L.s^{-1}$ and 138 $L.s^{-1}$. They do not model the water supply system. Therefore, they do not consider the energy needed to reheat the water. Moreover, a very optimistic COP of 5.2 was used for assumptions, which is very different of the COPs between 2 and 3.2 used by De Pasquale et al. [26] and Hubeck et al. [27].

For the city of Almere, the need for heating is very low, but the exchange model does not consider that the presence of pipes influences the ground temperature. For the city of Copenhagen [27], the degree of ground heat utilization (38%) is more than three times higher than that found by De Pasquale et al. (10.3%) in Milan [26].

This discrepancy can be explained by the difference in the thermal model used in the two studies (the undisturbed soil model used for Copenhagen overestimates the heat exchange between soil and pipes) and the water residence time in the pipes. A higher residence time increases the heat exchange between the pipes and the soil, thus leading to a higher degree of ground heat utilization. According to Hubeck et al. [27], the water residence time is higher in the Copenhagen network than in the Milan network.

1.3. Heat recovery for cooling

Less few studies consider only cooling applications. Van der Hoek et al. [31] identify cold production as an interesting use of drinking water networks. Guo and Hendel [32] study the use of water for cooling during heat waves. They considered several applications for cooling in Paris, such as cooling subway stations, producing ice for apartments cooling, and cooling streets by watering the roadway. For the subway stations cooling, the proposed solution could cool up to 240 stations in Paris with a temperature increase in the network of 1°C (Guo and Hendel [32]).

Van der hoek et al. [31] describe a cooling system with the drinking water networks of Amsterdam that serves the pharmaceutical process of the company Sansuin. The system has been

operational since 2018 and provides a portion of the company's cooling needs, reducing electricity consumption for cooling by a factor of ten.

The regulations requires that the temperature after the exchange remains below $15°C$. To maintain a sufficient temperature difference in the heat exchanger, the system operates when the network temperature is below $14°C$, which is typically from November to April. The exchanger is coupled to an energy storage system in an aquifer to take advantage of cooling with mains water all year round. The installation makes it possible to recover 5.6 GWh of cold per year and to reduce CO_2 emissions by 1,100 tonnes per year. In the future, production should increase to 11.1 $GWh.year^{-1}$ ([33]). In this case, the drinking water is heated, and the end-users reduce their energy consumption for hot water production

Despite studies on the utilization of water networks for heat exchange, there is currently no method for determining the global potential of these networks. Indeed, the studies that examine heat recovery from water systems only consider heat exchange at the inlet point of the network which limits the evaluation of the global thermal potential and the potentials' locations. To overcome this limitation, a new method was developed to assess the possibility of conducting multiple exchanges within the same network and to identify potential locations. This method enables the evaluation of the thermal potential of the network for a single application (either heating or cooling) across the entire network. Indeed, the evaluation of the thermal potential for the combination of heat and cold applications requires adding constraints on the exchanges, such as a minimum distance between two exchanges. Without such constraints, the results would give an infinite potential consisting of an succession of heat and cold exchange of the same power at the same place.

1.4. Water temperature modeling

It appears that heat and cold recovery from water supply systems are promising, but a better evaluation of the temperature in the networks is necessary to reduce the number of assumptions made in the calculation. Additionally, the temperature changes after the exchanges affect the systems' efficiencies, leading to the need for end-users to reheat the water.

Water temperature in networks has been widely studied to assess water quality. Agudelo-Vera et al. [34] conducted a comprehensive a literature review on the modeling of water temperature in networks. EPANET-MSX software was used to model temperature in water networks by Blokker et al. [25], De Pasquale et al. [26], Hubeck-Graudal et al. [27] and Hypolite et al. [35]. However, the results obtained in these studies vary based on the choice of heat exchange model between the pipes and the ground. De Pasquale et al. [26] and Hypolite et al. [35] compare exchange models from the literature. They show the importance of considering the impact of pipes on soil temperature around the pipes. Furthermore, Hypolite et al. [35] proposed a novel approach that takes into account the dynamic aspect of the heat exchange between the pipes and the soil.

2. Materials and methods

2.1. Network description

The Canal de Provence water network is used to illustrate the method. The Canal de Provence is a raw water network made up of 5,600 km of buried pipes that transport 200 million cubic meters of raw water per year [36].

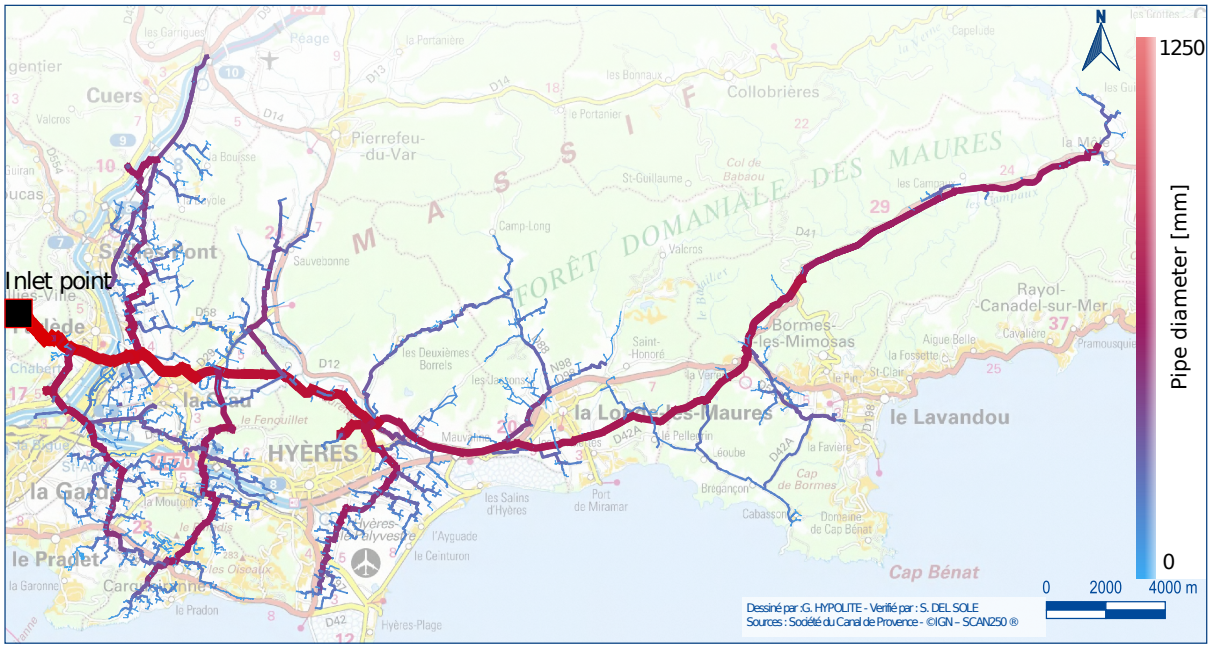

Figure 1: Map of the A network, colors and lines thickness representing the pipe diameter

A dozen micro-power plants representing a power of 3.8 MW are installed on the canal de Provence network. These plants produce 12 $GWh.year^{-1}$ of hydroelectricity. The method is demonstrated on a portion of the network referred to as network A, which is located east of the city of Toulon in southern France and consists of 460 km of pipes with one entry point (as shown in Figure 1). The model was also applied to a second sub-section (called network B), consisting of 205 km of pipes with two entry points and located northeast of the city of Marseille in southern France. These two networks were selected due to their size and significant flow.

2.2. Influence of heat exchanges on the network

The system that is considered for thermal recovery on water system is described in figure 2 Depending on the application and the required temperature level, the exchange system can be a reverse cycle machine (heat pump or refrigeration machine) or a direct exchange. For hydropower production, the systems that can be used are turbine or PAT. These system has been widely described in the literature and will not be discuss further here.

In the pipe, the water is initially at the temperature T_i. It is then heated or cooled in the system to the return temperature T_o. The diverted flow is then re-injected into the pipe, where after mixing, the water temperature becomes T_m. The flow in the supply line (before the bypass) is noted $\dot{m}$,

the diverted flow is noted $\dot{m}_d$. The energy exchanged in the system ($\dot{Q}$) is given by equation 1. C_{p_e} is the heat capacity of water. Here, it is assumed that the heat exchange is not limited by the user's temperature, which is equivalent to assume that the user's temperature is below T_o for cooling applications and above for heating applications.

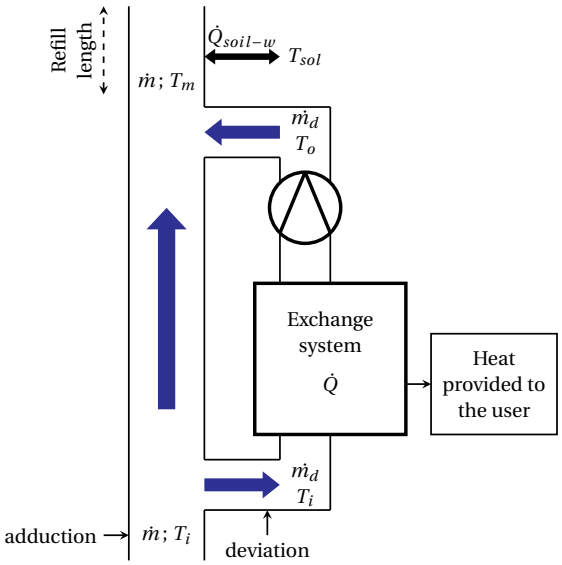

Figure 2: Schematic diagram of the valorization system for heat recovery

$$\dot{Q} = \dot{m} \cdot C_{p_w} \cdot (T_m - T_i) \tag{1}$$

The temperature after mixing is fixed; therefore, the thermal power depends on the water flow rate and temperature. In the network, the temperature of the water tends to approach that of the surrounding ground. It is then possible to make a new exchange after a certain distance.

For water flow and temperature determination in the water system, the hydraulic and thermal model by Hypolite et al. [35] is used. User profiles are defined to evaluate the flows. If for some users, the consumption is known with hourly precision, for others, the hourly consumption is estimated based on a weighted average of the total consumption The hydraulic calculation is performed using the Epanet software [29]. The thermal model uses the method of Barletta et al. [37] for calculating the heat exchange between the soil surface and the pipe. Barletta's method introduces two coefficients that account for the temporal variability of the soil surface temperature. It uses a form factor to evaluate the impact of pipes on soil temperature. The differential equation governing the evolution of the temperature is solved with Epanet MSX [30]. The soil surface temperature, which is a boundary condition, is obtained from satellite measurements [38]. The model allows the addition of heat exchanges on the network by adding a source term to the energy balance of the node as shown in equation 2.

$$h^{i;x=0} = \frac{\sum_j Q_j h^{j;x=l} + S/\rho}{\sum_j Q_j} \tag{2}$$

Equation 3 gives the relation between the value of the source term and the water temperature after heat exchange. Therefore, the source term (S) can be directly specified or calculated using equation 3 by setting the desired water temperature after the exchange.

$$T_o = T_i + \frac{S}{\dot{m} \cdot C_p} \tag{3}$$

For heating, the network serves as a cold reservoir, and the source term is negative $S < 0$. According to the equation 3, the water temperature decreases during heat exchange. For cooling, the network serves as a hot reservoir, the source term is positive $S > 0$, and the temperature increases during the exchange.

2.3. Network's energy potential calculation

The proposed method to evaluate the energy potential of the network is based on a model of the network on Epanet and Epanet MSX. Pressure and flow values are used to calculate hydropower potential, while temperature and flow values are used for thermal potential calculations. The algorithm described in this section is implemented in Matlab, and the code can be found on GitHub

The method consists of the following steps: (i) computing the available energy on the entire network, which is the energy that can be extracted from the network while maintaining its normal operation,i.e. , keeping a sufficient pressure for hydraulic application and keeping the temperature in an acceptable range for thermal application; (ii) identifying the location with the maximum available energy value and adding a turbine or a heat exchange at that location; (iii) re-evaluating the network's potential with the turbine or heat exchange and finding the second-best location; (iv) evaluating the maximum exchange potential iteratively adding turbines or exchanges to the network.

The expressions for thermal and hydro power have the same form. In both cases, the power is proportional to the mass flow rate multiplied by a difference in a physical quantity (pressure for hydro and temperature for thermal). Hence, a similar method can be used for both

Thermal- and hydro-power expression have the same form. In both cases, the power is proportional to the mass flow rate multiplied by a difference in a physical quantity (pressure for hydro and temperature for thermal). Hence, a similar method can be used hydraulic, heating, or cooling applications. For hydroelectricity production, adding a turbine will decrease the pressure downstream. The pressure is reduced by the turbine pressure drop at all the downstream points. Adding a heat exchange will change the temperature downstream. In this case, the temperature change is not the same everywhere as it depends on the water temperature. We will first present the hydraulic calculation. Then, the necessary modifications for the thermal calculation (to take into account the influence of temperature on temperature change) will be exposed.

2.3.1. Hydraulic potential

The hydraulic potential is the hydraulic energy that can be extracted from the network, keeping the required pressure at any node in the network.

2.3.1.1. Available pressure calculation. At a given node (n) in the network, the available pressure $\Delta P_a(n)$ is the difference between the actual pressure and the pressure necessary to operate the network. The pressure available for node n at time t is given by equation 4.

$$\Delta P_a(n,t) = \min\left(\min_{n_i \in ns(n,t)} \left(\Delta P_a(n_i,t) - DP_{n-n_i}(t) \right), P(n,t) - P_r(n,t) \right) \tag{4}$$

$ns(n,t)$ is the set of nodes that are directly downstream of node n at time t (directly means that a single pipe segment separates the nodes). Since the direction of water circulation in the network can change over time, the set of downstream nodes is time-dependent and must be calculated for each time step. DP_{n-n_i} is the head loss in the pipe segment between nodes n and n_i. $P(n)$ is the pressure at node n. $P_r(n)$ is the minimum required pressure at node n : for delivery node (node with consumption), P_r is a contract value (consumer dependent), for the other nodes the value is set to avoid a depression in the pipes ($P_r = 10^5\ Pa$).

To calculate the available pressure at a node, knowledge of the available pressure downstream of that node is required. A recursive method is used for the calculation. If a node has no downstream nodes, meaning that it is at the end of the network, the available pressure is given by equation 5.

$$\Delta P_a(n,t) = P(n,t) - P_r(n,t) \tag{5}$$

The calculation is performed by calling the recursive function for input nodes and for tanks.

2.3.1.2. Available power calculation. Equation 6 gives the mechanical energy that can be extracted at node n.

$$\dot{W}(n,t) = \rho_w \cdot \dot{m}(n,t) \cdot \Delta P_a(n,t) \tag{6}$$

$\dot{W}$ is the turbine power, and $\dot{m}$ is the mass flow of fluid entering the node. Integration of the power over time gives the energy potential (eq. 7).

$$E(n) = \int_{t_0}^{t_f} \dot{W}(n,t) \cdot dt \tag{7}$$

2.3.1.3. Algorithm. The energy potential is computed for each node in the network. The algorithm finds the network node with the largest potential and adds a turbine to this node. Adding a turbine to the network will modify the potential of the other nodes. The potential is modified for two reasons: (i) the pressure downstream of the turbine node will be reduced, leading to a reduction of potential for these points, and (ii) the available pressure for upstream nodes could also be reduced, as decreasing the pressure at these nodes will reduce the pressure at the turbine node. Therefore, the network's pressure and the hydraulic potential are recalculated before adding another turbine. The calculation is repeated as long as the potential is higher than a fixed value (E_{min}). Adding the turbine reduces the downstream pressure by ΔP_t. Upstream, the necessary pressure must be recalculated.

The algorithm for hydraulic potential calculation is shown in figure 3, 4, 5, 6.

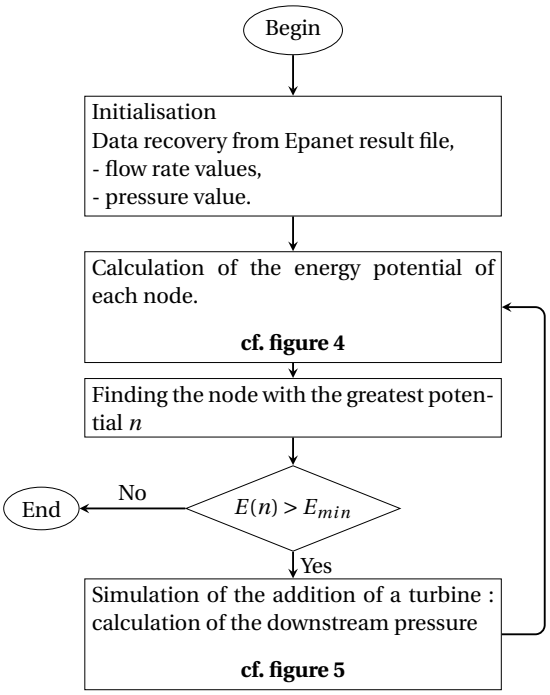

Figure 3: Algorithm for calculating the water network hydraulic potential.

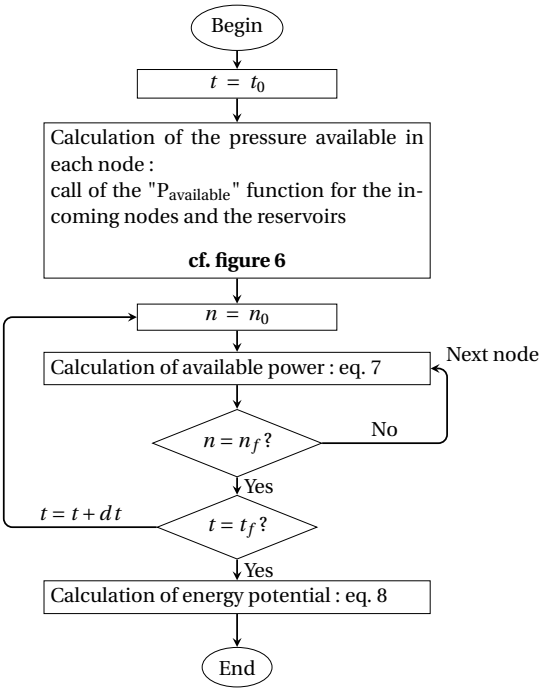

Figure 4: Algorithm for calculating the hydraulic potential for each nodes of a network

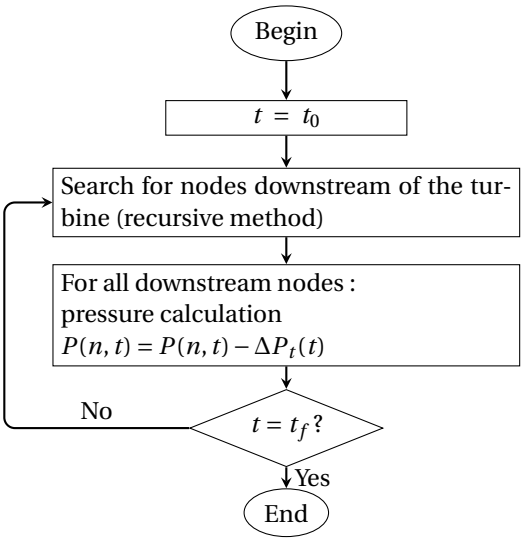

Figure 5: Algorithm for simulating the addition of a turbine.

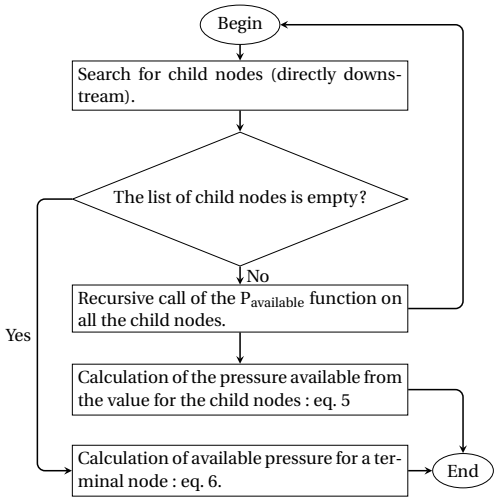

Figure 6: Algorithm for the pressure calculation

2.3.2. Heat potential

A calculation similar to the hydrodynamic calculation is performed to evaluate the network's thermal potential. In this case, the temperature evolution in pipes depends on the water temperature (as the heat exchange between the pipes and the ground is influenced by on the water temperature). The heat $\dot{Q}$ that can be exchanged at a node n is given by equation 8a. Integration of heat over time gives the available energy (equation 8b).

$$\dot{Q}(n,t) = \dot{m}(n,t) \cdot C_p \cdot \Delta T_a(n,t) \tag{8a}$$

$$E(n) = \int_{t_0}^{t_f} \dot{Q}(n,t)dt \tag{8b}$$

The available temperature ΔT_a at a node in the network is given by equation 9a if the node is not terminal, and by equation 9b if it is terminal. T_r is the temperature limit in the network. For heating applications, this is the minimum allowable temperature (T_{min}); for refrigeration applications, this is the maximum allowable temperature (T_{max}).

$$\Delta T_a(n,t) = \min\left(\min_{n_i \in ns(n,t)} \left(\Delta T_a(n_i,t) - DT_{n-n_i}\right), |T(n,t) - T_r(n,t)|\right) \tag{9a}$$

$$\Delta T_a(n,t) = |T(n,t) - T_r(n,t)| \tag{9b}$$

DT_{n-n_i} is the temperature difference between the inlet and the outlet of a pipe. This value depends on the temperature of the water in the pipe. $(n - n_i)$ refers to the pipe between the nodes n and n_i The calculation of this parameter is given by equation 10.

$$DT_{n-n_i} = \frac{T_{water} - T_\infty(n - n_i, t)}{\dot{m}(n - n_i, t) \cdot C_p \cdot R_{tot}(n - n_i, t)} \tag{10}$$

The values of total thermal resistance (R_{tot}), water flow ($\dot{m}$) and exchange temperature (T_∞) are obtained from the thermal and hydraulic calculations [35]. The water temperature for the calculation of the exchange (T_{water}) is assumed to be equal to the average temperature of the water entering and leaving the pipe.

The calculation for the simulation of the exchanger addition is similar to the hydrodynamic calculation, with the new temperature calculation considering equation 10 The algorithm presented in figures 3, 4 and 6 is repeated by replacing the available pressure with the available temperature. The algorithm in figure 5 is modified to take into account the calculation of the heat exchange (eq. 10), the new algorithm is presented in the figure 7. Differences with the hydraulic calculation are marked in red.

2.4. Hypothesis

This study only focuses on pressurized water systems, and therefore cannot be applied to open channels. The calculation of hydropower in open channels is entirely different and cannot be adapted from our method. However, the calculation of thermal potential can be adapted, but a model for heat exchange between water and air must be added.

The hypotheses made for the energy potential calculation are of two types: (i) hypotheses on network hydraulic and thermal modeling and (ii) hypotheses on the calculation of energy potential from the results of the modeling.

The hypotheses regarding network hydraulic and thermal modeling are described in detail in a previous study [35]. The main hypotheses regarding pressure and flow calculation are based on the distribution of water consumption throughout the year. The flow for some consumers is measured, but for others, only the annual consumption is known. The modeling results have been validated against measurements and a maximum difference of 10% on the water flow has been observed for an entire year. The temperature calculation uses a model that computes heat exchange between the soil and pipes, which assumes a periodic variation of the soil surface temperature. This variation was determined using satellite-measured temperatures. The hypothesis on the thermal model has

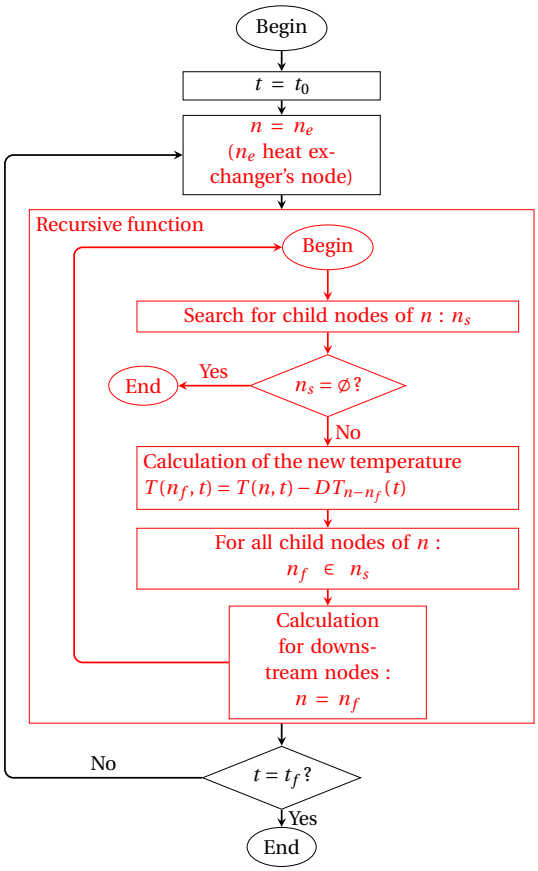

Figure 7: Algorithm for simulating the addition of a heat exchanger. The differences with the hydraulic calculation are marked in red.

been validated with measurements of the water temperature, with a root mean square error of $0.84°C$ for a year.

For the energy potential calculation, the hypothesis is based on the location of the turbine (or heat exchanger). The equipment is placed at the location with the highest potential for the calculation.

2.5. Data and software availability

Original data of this study including water temperature, pressure and flow according to time are available at Mendeley Data [39].

3. Results and discussions

3.1. Hydraulic potential

The hydrodynamic potential has been calculated for the two sub-network A and B. The algorithm is applied to find the five highest potentials in each networks. For network A (see figure 1) the potential is 6.97 $GWh.year^{-1}$,which is the sum of the five potentials presented in figure 1. The potential of network A corresponds to an average power of 795 kW. For network B, the potential

is 3.05 $GWh.year^{-1}$. These values , as well as the networks' lengths and flows, are summarized in table 1.

	Constraint	Network A		Network B		Total Network	
Size	-	469 km		205 km		5600 km	
Mean inlet flow rate	-	1136 $L.s^{-1}$		260 $L.s^{-1}$		6000 $L.s^{-1}$	
Max inlet flow rate	-	2659 $L.s^{-1}$		1004 $L.s^{-1}$		-	
Min inlet flow rate	-	14 $L.s^{-1}$		73 $L.s^{-1}$		-	
Hydraulic	-	6.97 GWh	795 kW	3.05 GWh	348 kW	-	-
Heating	$T_{min} = 4°C$	775 GWh	88 MW	310 GWh	35 MW	6478 GWh	740 MW
Cooling	$T_{max} = 25°C$	359 GWh	41 MW	137 GWh	16 MW	2961 GWh	338 MW
Cooling	$T_{max} = 35°C$	561 GWh	64 MW	218 GWh	25 MW	4651 GWh	531 MW

Table 1: Potentials for energy recovery for the year 2018. For each network, the left column gives the energy potential in GWh per year; the right column gives the corresponding average power in MW. Values for the total network are obtained by extrapolating the sub-networks value over the total length of pipes.

The map in figure 8 shows the potential distribution on network A. The available power varies linearly with flow rate and is thus concentrated on the main lines where flow is significant. However, the available pressure is highly dependent of the location on the network. It is, therefore, challenging to predict *a priori* the location of high potentials. The calculation allows highlighting these locations.

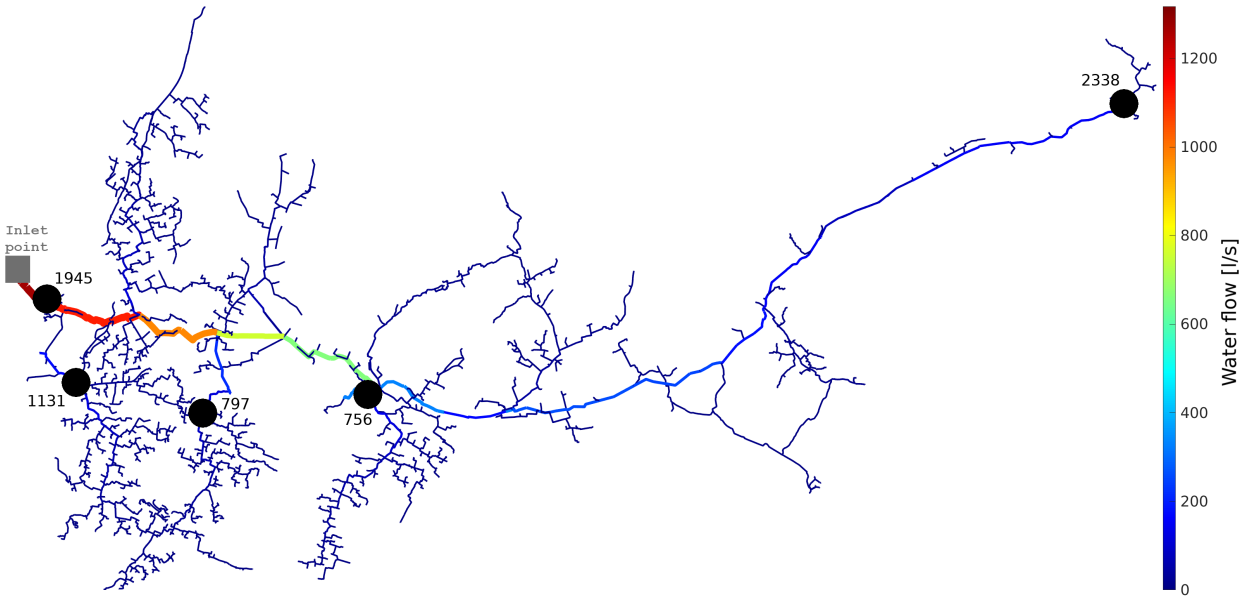

Figure 8: Water flow in network A on June 30 and distribution of hydraulic potential (black circles; the associated values are in MWh/year).

Figure 9 shows the available power evolution over time for the 3 locations with the most significant potential. The available power is highly variable, with important jumps. These jumps

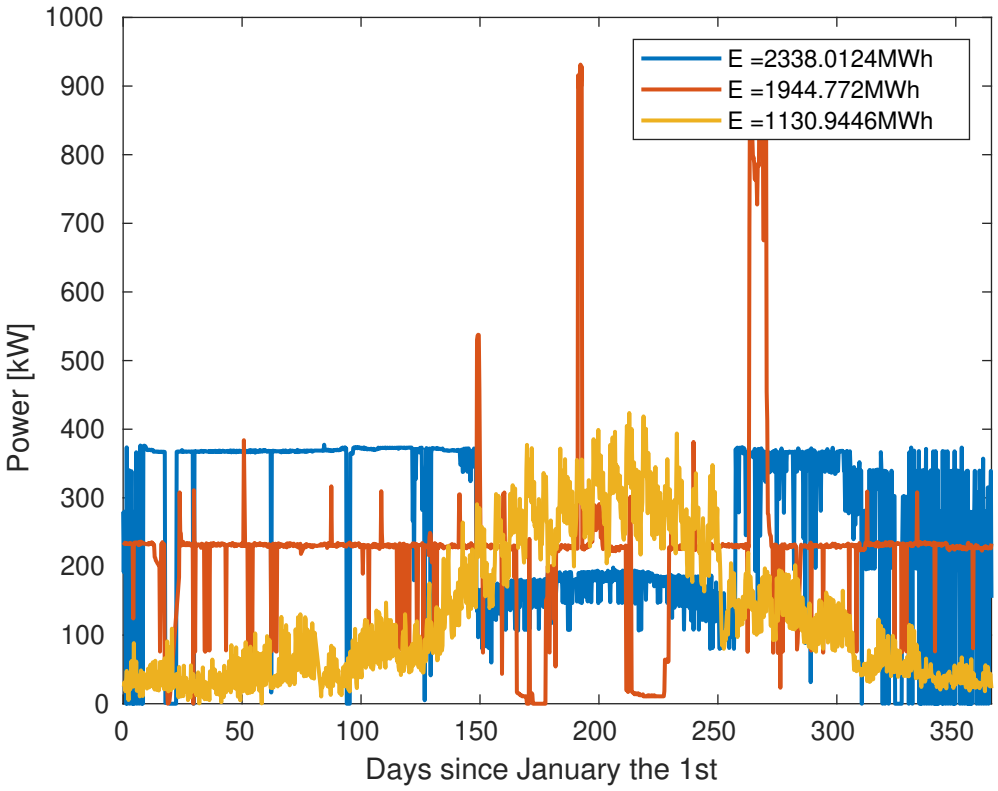

Figure 9: Hydraulic power exploitable on the network.

and variations are primarily due to the flow variation in the pipes, which is imposed by consumers' demand. One of the difficulties for turbine installation at these locations is the temporal variability of the available power.

The potential for hydroelectricity production in canal de Provence is already largely exploited. A plant is installed at the locations of network A with the potential of 1945 $MWh.year^{-1}$. The location with the 2338 $MWh.year^{-1}$ is currently being studied for a micro-power plant installation. The method then allows finding the points with high potential that had already been identified from the flow and pressure values. Furthermore, it highlights smaller potentials that were previously unidentified.

As far as the authors are aware, there have been no studies that have evaluated the total energy potential for hydropower recovery from water supply systems. As a result, it is not currently possible to compare our findings with existing literature. Furthermore, our results are highly dependent on the specific characteristics of the water network, such as the mean flow rate and elevation profile. The values generated by the algorithm represent the total amount of recoverable energy, which represents a theoretical maximum. To actually recover this energy, it is necessary to extract the maximum power at any given moment. As a result, the primary benefit of this method is to identify strategic locations within a network model for the production of hydroelectricity.

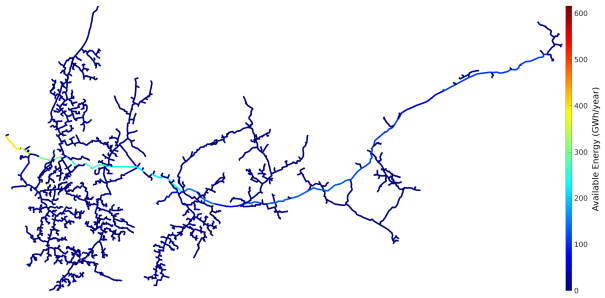

Figure 10: Network A layout colored according to the available thermal energy for heating (with $T_{min} = 4°C$).

3.2. Heat and cold potential

We simulate an exchange of 1.5 MW to understand the recovery mechanism in pipes after heat exchange. The increase in water temperature coming from the canal is of the order of $3°C$ (depending on the water flow). In pipes, the exchange with the ground tends to bring the temperature back to the initial value. In the mainline, the water temperature is influenced over a long distance. The water is heated by at least $1°C$ over 10 km downstream of the exchange. Indeed, these pipes have a large diameter ($d > 500$ mm), and the length to reach a given temperature depends on the square of the diameter ([35]). In smaller pipes, the water reaches ground temperature before the delivery nodes.

The available thermal energy for heating applications of the initial system has been calculated with equation 8, the minimum temperature is $T_{min} = 4°C$. Figure 10 shows the available energy in the water system. The available energy linearly depends on the flow. It is then concentrated in the large-diameter pipes in which high water flows circulate. This potential represents a few hundred gigawatt-hours per year. This figure highlights both the very significant potential and the unequal distribution of this potential on the network. Finally, figure 10 shows the location with sufficient power to identify potential users.

The calculation of thermal potentials has been performed for both networks. The potentials are computed as long as they are higher than 1 $GWh/year$.

For heating, the temperature constraint is set at $4°C$, while for cooling, it is set at $25°C$. Table 1 summarizes the thermal potential values, which vary depending on the application (heating or cooling) and the temperature constraint imposed. The network has a potential of several hundred gigawatt-hours per year. Table 1 also presents the associated annual average power values.

For the two sub-networks A and B, the ratio of the potential to the length of the pipeline is similar. Assuming that this ratio is the same for all 5 600 km of pipelines, the sub-networks' potential is extrapolated to estimate the total system potential. The column concerning the complete network presents the extrapolated values. The value of the temperature constraint has a strong influence on the thermal potential; increasing the constraint by $10°C$ thus increases the potential by 60%.

Figure 11 then shows the distribution of the locations with the highest potential (and the corresponding value). The potential is concentrated at the inlet point where the entire flow passes. If an exchange is made there, the water enters the network at the temperature limit. The remaining

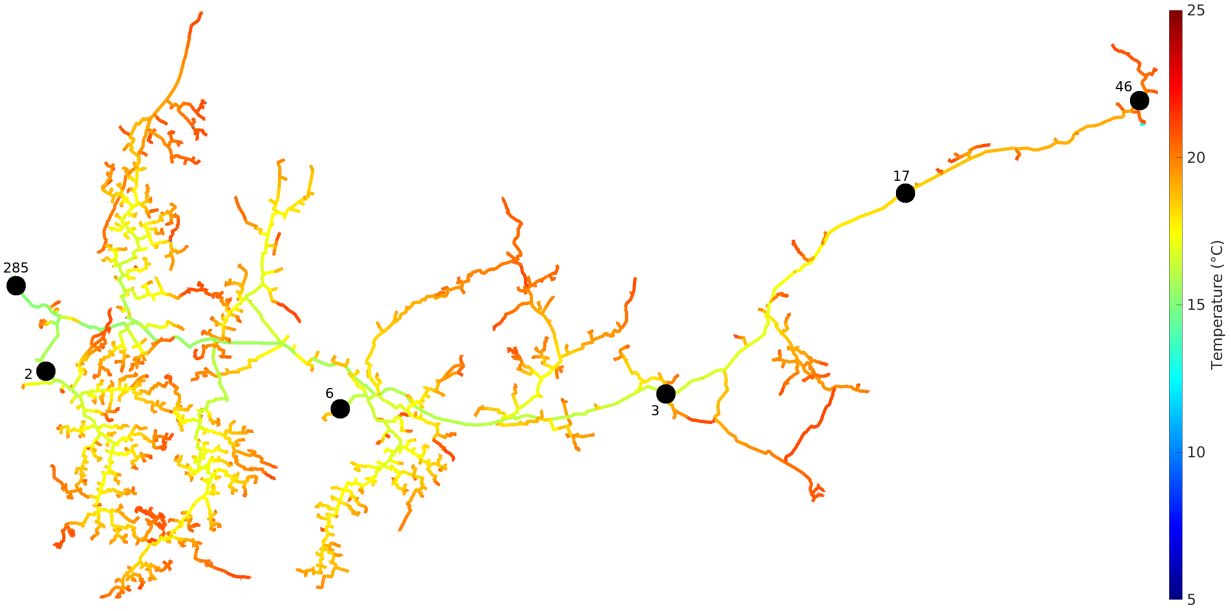

Figure 11: Water temperature in network A on June 30 and distribution of thermal potential (black circles; the associated values are in GWh/year).

heat that can be extracted corresponds to the exchange between the pipes and the soil. This heat is small compared to the potential of the water entering the network (20 % of the total potential).

The temporal evolution of the three most significant potentials is presented in figure 12 (the values in the legend of figure 12 correspond to the potentials displayed in figure 11). The potential's temporal variability significant, making it necessary to find users whose needs match the available power to get the most out of the potential.

As for the total hydro-potential, there are currently no established methods in the literature for evaluating the total thermal potential of a water system. In comparison of value from Table 1, the heat recover in the case study of the city of Copenhagen [25] is $11,5 GWh.year^{-1}$, it is $4.8 GWh.year^{-1}$ in the case study of Milan[26], and it is $3.9 GWh.year^{-1}$ in the case of Głogów [28]. Furthermore, the cooling application using the Amsterdam water system allows for the recovery of $5.6 GWh$ of cold per year, which is expected rise to $11.1 GWh.year^{1}$ in the future. These values are significantly lower when compared to those in Table 1, This is because these studies only evaluate the water at the inlet of the network, and do not provide a comprehensive evaluation of the entire water system's potential. In their study, Ahmad et al. [40] determined the retrievable thermal energy for cooling based on the drinking water flow rate in the heat exchanger and the constraint on the return temperature. The inlet water temperatures used in their study are for the years 2018 and 2019 and are slightly ($2°C$ to $3°C$) lower than the values observed in our case. They only considered a single exchange and did not compute the entire network potential. Therefore, the value they obtained can be compared to the potential at the inlet point of our network. In our case, a potential of $285 GWh.year^{-1}$ can be recovered at this point with a mean water flow rate of $1136 L.s^{-1}$ (cf. Figure 12). The value from Ahmad et al. [40] for the same water flow rate and

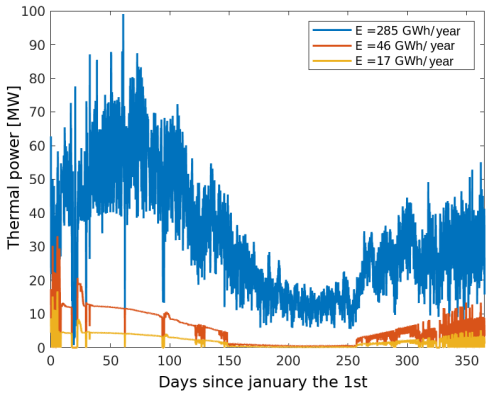

Figure 12: Thermal power that can be recovered on network A for cooling with $T_{max} = 25°C$. The legend value correspond to the potentials displayed in figure 11

temperature constraint is 498 $GWh.year^{-1}$. This value is almost twice the one obtained in our case, which can be explained by the fact that they assumed a constant water flow rate, while the flow rate is variable in our network. In particular, in the case of the Canal de Provence, the water flow is much larger in the summer due to irrigation, which corresponds to higher water temperatures that are less favorable for cooling purposes. This highlight the importance of considering the temporal variability of water flow for potential calculation.

4. Conclusion

The results presented in this study estimate the energy potential of a water supply system, i.e., the maximum amount of energy that can be extracted from the network while respecting the constraints of maintaining a low and high temperature of the water. The only input required for the calculation are the network calculation result files, which makes the method easily applicable to other networks.

The hydraulic calculations show potentials of respectively 7 $GWh.year^{-1}$ and 3 $GWh.year^{-1}$ for sub-networks of respective lengh of 469 km and 205 km.

The thermal potential values obtained were extrapolated over the entire 5 600 km of pipelines. The total potential is several hundred megawatts for the production of heat or cold. The available energy is 6478 $GWh.year^{-1}$ for heating and 2961 $GWh.year^{-1}$ for cooling.

However, exploiting these potentials could be challenging due to the temporal variability of the available power and the distribution of the potential on the networks. In this study, we have developed a tool to estimate and locate the interesting potentials for the installation of exchangers or hydroelectric power stations without *a priori* knowledge of the network.

Although the available power is significant, it is not evenly distributed over the network. In the search for the adequacy between the users' needs and the resource, it is thus important to consider the geographical aspect. Especially, the distance between the users and the resource must remain sufficiently small. This limitation is of economic order; the cost of the pipes between the users and the water system must be offset by the energy savings realized. Therefore, the acceptable distance will depend on both the installation cost and the exchange power.

The calculation only evaluates the thermal potential for a given application (heating or cooling). It may be interesting to consider coupling these applications by alternating heat and cold production. This type of application involves the notion of synergy between users. The succession between the types of use could considerably increase the network's potential provided that good consistency between the applications is ensured. The evaluation of the thermal potential for the simultaneous use of heat and cold applications involves determining the optimal distribution of heat and cold supply in a given network. This is a perspective of this work that can be achieved by adding the addition of constrains on the exchanges.

References

[1] Alexandru Andreï, Simon Beck,, Amanda Don Mahawattege,, Alexis Foussard, Rachida Laghouati,, Jean Lauverjat, Thomas Merly-Alpa,, Évelyne Misak, Cécile Phan,, Corentin Plouhinec, Jean-Philippe Rathle,, Olivier Ribon, Nicolas Riedinger, Chiffres clés de l'énergie - Édition 2021, Tech. rep., Le service des données et études statistiques (SDES) (2021).

[2] O. Ruhnau, L. Hirth, A. Praktiknjo, Time series of heat demand and heat pump efficiency for energy system modeling, Scientific Data 6 (1) (2019) 189. doi:10.1038/s41597-019-0199-y.

[3] B. Bach, J. Werling, T. Ommen, M. Münster, J. M. Morales, B. Elmegaard, Integration of large-scale heat pumps in the district heating systems of Greater Copenhagen, Energy 107 (2016) 321–334. doi:10.1016/j.energy.2016.04.029.

[4] B. Coelho, A. Andrade-Campos, Efficiency achievement in water supply systems—A review, Renewable and Sustainable Energy Reviews 30 (2014) 59–84. doi:10.1016/j.rser.2013.09.010.

[5] M. Wakeel, B. Chen, Energy Consumption in Urban Water Cycle, Energy Procedia 104 (2016) 123–128. doi:10.1016/j.egypro.2016.12.022.

[6] K. M. Twomey, M. E. Webber, Evaluating the Energy Intensity of the US Public Water System, in: ASME 2011 5th International Conference on Energy Sustainability, American Society of Mechanical Engineers Digital Collection, 2012, pp. 1735–1748. doi:10.1115/ES2011-54165.

[7] Y. Liu, M. S. Mauter, Marginal energy intensity of water supply, Energy & Environmental Science 14 (8) (2021) 4533–4540. doi:10.1039/D1EE00925G.

[8] N. Fontana, M. Giugni, D. Portolano, Losses Reduction and Energy Production in Water-Distribution Networks, Journal of Water Resources Planning and Management 138 (3) (2012) 237–244. doi:10.1061/(ASCE)WR.1943-5452.0000179.

[9] H. M. Ramos, Energy efficiency in a water supply system: Energy consumption and CO2 emission 3 (3) (2010) 10.

[10] R. Sitzenfrei, D. Berger, W. Rauch, Design and optimization of small hydropower systems in water distribution networks under consideration of rehabilitation measures, Urban Water Journal 15 (3) (2018) 183–191. doi:10.1080/1573062X.2015.1112410.

[11] G. Rabinowitz, A. Mehrez, A. Rabina, A Nonlinear Heuristic Short-Term Model for Hydroelectric Energy Production: The Case of the Hazbani-Dan Water System, Management Science 38 (3) (1992) 419–438. doi:10.1287/mnsc.38.3.419.

[12] J. García Morillo, A. McNabola, E. Camacho, P. Montesinos, J. Rodríguez Díaz, Hydro-power energy recovery in pressurized irrigation networks: A case study of an Irrigation District in the South of Spain, Agricultural Water Management 204 (2018) 17–27. doi:10.1016/j.agwat.2018.03.035.

[13] E. Cabrera, M. A. Pardo, R. Cobacho, E. Cabrera, Energy Audit of Water Networks, Journal of Water Resources Planning and Management 136 (6) (2010) 669–677. doi:10.1061/(ASCE)WR.1943-5452.0000077.

[14] S. Spedaletti, M. Rossi, G. Comodi, D. Salvi, M. Renzi, Energy recovery in gravity adduction pipelines of a water supply system (WSS) for urban areas using Pumps-as-Turbines (PaTs), Sustainable Energy Technologies and Assessments 45 (2021) 101040. doi:10.1016/j.seta.2021.101040.

[15] H. Ramos, A. Borga, Pumps as turbines: An unconventional solution to energy production, Urban Water 1 (3) (1999) 261–263. doi:10.1016/S1462-0758(00)00016-9.

[16] A. Muhammetoglu, I. E. Karadirek, O. Ozen, H. Muhammetoglu, Full-Scale PAT Application for Energy Production and Pressure Reduction in a Water Distribution Network, Journal of Water Resources Planning and Management 143 (8) (2017) 04017040. doi:10.1061/(ASCE)WR.1943-5452.0000795.

[17] C. Tricarico, M. S. Morley, R. Gargano, Z. Kapelan, D. Savić, S. Santopietro, F. Granata, G. de Marinis, Optimal energy recovery by means of pumps as turbines (PATs) for improved WDS management, Water Supply 18 (4) (2018) 1365–1374. doi:10.2166/ws.2017.202.

[18] M. De Marchis, G. Freni, Pump as turbine implementation in a dynamic numerical model: Cost analysis for energy recovery in water distribution network, Journal of Hydroinformatics 17 (3) (2015) 347–360. doi:10.2166/hydro.2015.018.

[19] M. De Marchis, C. Fontanazza, G. Freni, A. Messineo, B. Milici, E. Napoli, V. Notaro, V. Puleo, A. Scopa, Energy Recovery in Water Distribution Networks. Implementation of Pumps as Turbine in a Dynamic Numerical Model, Procedia Engineering 70 (2014) 439–448. doi:10.1016/j.proeng.2014.02.049.

[20] M. Mohammadi, M. Yasi, S. Jamali, H. Hajikandi, Optimal location for installing small hydropower plant on water supply pipelines, Proceedings of the Institution of Civil Engineers - Energy 172 (2) (2019) 64–78. doi:10.1680/jener.18.00026.

[21] Y. Cho, R. Yun, A raw water source heat pump air-conditioning system, Energy and Buildings 43 (11) (2011) 3068–3073. doi:10.1016/j.enbuild.2011.07.028.

[22] S. Oh, Y. Cho, R. Yun, Raw-water source heat pump for a vertical water treatment building, Energy and Buildings 68 (2014) 321–328. doi:10.1016/j.enbuild.2013.09.011.

[23] Ş. Kılkış, Transition towards urban system integration and benchmarking of an urban area to accelerate mitigation towards net-zero targets, Energy 236 (2021) 121394.

[24] G. Fambri, A. Mazza, E. Guelpa, V. Verda, M. Badami, Power-to-heat plants in district heating and electricity distribution systems: A techno-economic analysis, Energy Conversion and Management 276 (2023) 116543.

[25] E. J. M. Blokker, A. M. van Osch, R. Hogeveen, C. Mudde, Thermal energy from drinking water and cost benefit analysis for an entire city, Journal of Water and Climate Change 4 (1) (2013) 11–16. doi:10.2166/wcc.2013.010.

[26] A. M. De Pasquale, A. Giostri, M. C. Romano, P. Chiesa, T. Demeco, S. Tani, District heating by drinking water heat pump: Modelling and energy analysis of a case study in the city of Milan, Energy 118 (2017) 246–263. doi:10.1016/j.energy.2016.12.014.

[27] H. Hubeck-Graudal, J. K. Kirstein, T. Ommen, M. Rygaard, B. Elmegaard, Drinking water supply as low-temperature source in the district heating system: A case study for the city of Copenhagen, Energy 194 (2020) 116773. doi:10.1016/j.energy.2019.116773.

[28] J. Piotr, N. Elżbieta, Water pipe network as a heat source for heat pump integrated into a district heating, E3S Web of Conferences 22 (2017) 00210.

[29] L. A. Rossman, EPANET 2: Users manual (2000).

[30] F. Shang, J. G. Uber, L. A. Rossman, EPANET multi-species extension user's manual, Risk Reduction Engineering Laboratory, US Environmental Protection Agency, Cincinnati, Ohio (2008).

[31] J. P. van der Hoek, S. Mol, S. Giorgi, J. I. Ahmad, G. Liu, G. Medema, Energy recovery from the water cycle: Thermal energy from drinking water, Energy 162 (2018) 977–987. doi:10.1016/j.energy.2018.08.097.

[32] X. Guo, M. Hendel, Urban water networks as an alternative source for district heating and emergency heat-wave cooling, Energy 145 (2018) 79–87. doi:10.1016/j.energy.2017.12.108.

[33] Smart cooling system for pharmaceutical processes, http://www.cityzen-smartcity.eu/ressources/heating-and-cooling/smart-cooling-and-heating-systems-for-pharmaceutical-processes/ (Sep. 2016).

[34] C. Agudelo-Vera, S. Avvedimento, J. Boxall, E. Creaco, H. de Kater, A. Di Nardo, A. Djukic, I. Douterelo, K. E. Fish, P. L. Iglesias Rey, N. Jacimovic, H. E. Jacobs, Z. Kapelan, J. Martinez Solano, C. Montoya Pachongo, O. Piller, C. Quintiliani, J. Ručka, L. Tuhovčák, M. Blokker, Drinking Water Temperature around the Globe: Understanding, Policies, Challenges and Opportunities, Water 12 (4) (2020) 1049. doi:10.3390/w12041049.

[35] G. Hypolite, J.-H. Ferrasse, O. Boutin, S. Del Sole, J.-F. Cloarec, Dynamic modeling of water temperature and flow in large water system, Applied Thermal Engineering 196 (2021) 117261. doi:10.1016/j.applthermaleng.2021.117261.

[36] Société du Canal de Provence, http://www.canal-de-provence.com/Accueil/tabid/36/language/fr-FR/Default.aspx (2020).

[37] A. Barletta, E. Zanchini, S. Lazzari, A. Terenzi, Numerical study of heat transfer from an offshore buried pipeline under steady-periodic thermal boundary conditions, Applied Thermal Engineering 28 (10) (2008) 1168–1176. doi:10.1016/j.applthermaleng.2007.08.004.

[38] Z. Wan, S. Hook, G. Hulley, MOD11A1 MODIS/Terra Land Surface Temperature/Emissivity Daily L3 Global 1km SIN Grid V006 [Data set], NASA EOSDIS Land Processes DAACdoi:10.5067/MODIS/MOD11A1.006.

[39] G. Hypolite, Evaluation of a water network's energy potential in dynamic operation, mendeley data 1, publisher: Mendeley. doi:10.17632/jvczk66p36.1.
URL `https://data.mendeley.com/datasets/jvczk66p36`

[40] J. I. Ahmad, S. Giorgi, L. Zlatanovic, G. Liu, J. P. van der Hoek, Maximizing Thermal Energy Recovery from Drinking Water for Cooling Purpose, Energies 14 (9) (2021) 2413.